

NMR and local-density-approximation evidence for spiral magnetic order in the chain cuprate LiCu_2O_2

A. A. Gippius,¹ E. N. Morozova,¹ A. S. Moskvina,² A. V. Zalessky,^{3,*} A. A. Bush,⁴ M. Baenitz,⁵ H. Rosner,⁵ and S.-L. Drechsler⁶

¹Moscow State University, 119899, Moscow, Russia

²Ural State University, 620083, Ekaterinburg, Russia

³Institute of Crystallography, RAS, 117333, Moscow, Russia

⁴Moscow Institute of Radiotechnics, Electronics and Automation, 117464, Moscow, Russia

⁵Max Planck Institut für Chemische Physik fester Stoffe, D-01187, Dresden, Germany

⁶Leibniz-Institut für Festkörper- und Werkstoffforschung IFW Dresden, D-01171, Dresden, Germany

(Received 5 September 2003; revised manuscript received 30 April 2004; published 26 July 2004)

We report on ${}^6,{}^7\text{Li}$ nuclear magnetic resonance measurements of the spin-chain compound LiCu_2O_2 in the paramagnetic and magnetically ordered states. Below 24 K the NMR line shape shows a clear signature of incommensurate (IC) static modulation of the local magnetic field consistent with an IC spiral modulation of the magnetic moments. ${}^7\text{Li}$ NMR reveals strong phason-like dynamical fluctuations extending well below 24 K. A series of phase transitions at 24.2, 22.5, and 9 K is observed. Local density approximation based calculations of exchange integrals reveal a large in-chain frustration leading to a magnetical spiral.

DOI: 10.1103/PhysRevB.70.020406

PACS number(s): 75.10.Jm, 76.60.-k

Despite extensive efforts during the last decades spin ordering in frustrated $S=1/2$ quantum spin chains still remains a matter of broad activities.¹⁻⁶ Rich phase diagrams with commensurate (C) and incommensurate (IC) phases, with spin- and charge ordering, dimerization, or superconductivity have been predicted. Most studies have been focused on various cuprates with corner- or edge-shared CuO_4 plaquettes. Edge-sharing of CuO_4 plaquettes leads to CuO_2 chains with a nearly 90° Cu-O-Cu bond angle causing a reduced nearest neighbor (nn) transfer and a next-nearest neighbor (nnn) transfer of similar size allowing frustration effects. IC spiral states driven by ferromagnetic (FM) nn exchange and in-chain frustration have been predicted theoretically for CuO_2 chain compounds such as $\text{Ca}_2\text{Y}_2\text{Cu}_5\text{O}_{10}$ but discarded experimentally.^{5,6} The observation of in-chain IC effects in undoped quasi-one-dimensional cuprates is so far restricted by a sharp *magnetic field driven* C-IC transition observed in the spin-Peierls system CuGeO_3 at high magnetic fields.⁷ Here we report on ${}^6,{}^7\text{Li}$ nuclear magnetic resonance measurements (NMR) and local density (LDA) based analysis of the electronic and magnetic structure of the chain compound LiCu_2O_2 . We show that the observed spontaneous magnetic order can be described by a spiral modulation of the magnetic moments. Independently, LDA calculations and a subsequent Heisenberg-analysis reveal strong in-chain frustration driving spiral ordering in accord with the NMR data.

LiCu_2O_2 is an insulating orthorhombic compound^{1,8-10} with bilayers of edge-shared $\text{Cu}^{2+}\text{-O}$ chains running parallel to the b axis separated by Cu^{1+} planes. It exhibits a high-temperature antiferromagnetic (AFM)-like Curie-Weiss susceptibility $\chi(T)$. Low-temperature $\chi(T)$ and specific heat studies^{1,11} point to a series of intrinsic phase transitions at $T \approx 24.2$ K, $T \approx 22.5$ K, and $T \approx 9$ K pointing to a complex multi-stage rearrangement of the spin structure. Magnetization studies performed in external fields up to 5 T did not reveal any signatures of field-induced transitions. μSR data¹¹

point to a broad distribution of magnetic fields at the muon stopping sites. LSDA(+U) calculations point to a FM in-chain ordering.¹⁰ However, a simple FM ordering is in conflict with the μSR data¹¹ and the AFM dimer liquid picture.^{1,12} Thus, to settle origin and character of the spin ordering in LiCu_2O_2 further studies are required. NQR and NMR measurements being a local probe are standard tools to elucidate the electronic and the magnetic structure. However, the Cu NMR signal in LiCu_2O_2 stems presumably from non-magnetic Cu^{1+} ions¹³ and reflects mainly the disorder due to Li-Cu non-stoichiometry to be discussed elsewhere. We have performed ${}^6,{}^7\text{Li}$ NMR measurements on large single crystals¹⁴ at several temperatures both in the paramagnetic¹³ and in the ordered phases. The spectra were measured for two main orientations: $\mathbf{H} \parallel (\mathbf{a}, \mathbf{b})$ and $\mathbf{H} \perp (\mathbf{a}, \mathbf{b})$, and by 10° steps inbetween, by sweeping the magnetic field at a fixed frequency of 33.2 MHz, the signal was obtained by integrating the spin-echo envelope. In the paramagnetic state ($T = 45$ K) the ${}^7\text{Li}$ NMR line (Fig. 1) has a full width of 0.01 T (at the basement) and shows a typical (for a $I=3/2$ nucleus) first order quadrupole splitting pattern with $\nu_Q=51.7$ kHz. For $T < 24$ K a dramatic change of the ${}^7\text{Li}$ NMR line shape is observed. In general, the low- T NMR line shape shows a wide continuous symmetric distribution which evolution is presented in Fig. 2 for the $\mathbf{H} \parallel (\mathbf{a}, \mathbf{b})$ geometry. In the ordered phase we still deal with a strong and narrow central peak but with a well developed inhomogeneously broadened basement. Lowering T the central peak weakens and disappears near $T \approx 10$ K, while the basement gradually evolves into a well-defined sextet whose full width exceeds by a factor of 30(!) that of the paramagnetic phase. A similar situation takes place in $\mathbf{H} \perp (\mathbf{a}, \mathbf{b})$ geometry, but, with a specific quartet shape of the low- T saturated NMR spectrum (Fig. 3). Such spectra are unique signatures of an infinite number of non-equivalent Li sites. They correspond to an IC static modulation of local fields.¹⁵⁻¹⁷ To discriminate between mag-

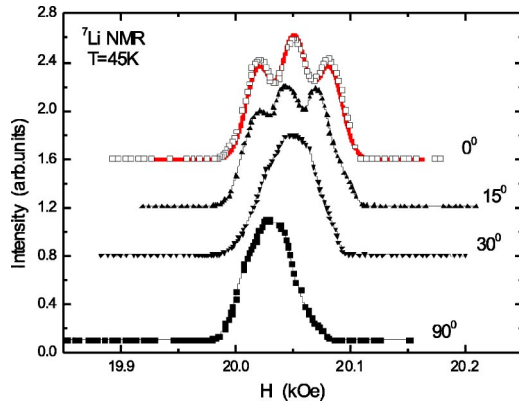


FIG. 1. (Color online) The ${}^7\text{Li}$ NMR spectrum at $T=45$ K for different orientations of the magnetic field with respect to the \mathbf{c} axis. The solid curve on the upper spectrum: our simulation.

netic and electric (quadrupole) effects we have performed parallel ${}^6\text{Li}$ NMR studies.¹⁸ The puzzling closeness of two NMR spectra below the critical temperature (Fig. 3, top panel) unambiguously points to a distribution of local magnetic fields as the origin of the observed phenomena. The additional local magnetic field $\mathbf{h}(\mathbf{R})$ seen by a nucleus at a site \mathbf{R} near a CuO_2 chain can be directly converted to a local spin polarization on the neighboring sites $\mathbf{S}(\mathbf{R}+\mathbf{r})$: $\mathbf{h}(\mathbf{R}) = \sum_r \hat{A}(\mathbf{r})\mathbf{S}(\mathbf{R}+\mathbf{r})$, where $\hat{A}(\mathbf{r})$ is the anisotropic tensor taking account of magnetic dipole and (super)transferred Li-Cu(O) hyperfine interactions. When $h \ll H_0$ (the uniform external magnetic field: $\mathbf{H}_0 = H_0(\sin \Theta \cos \Phi, \sin \Theta \sin \Phi, \cos \Theta)$):

$$h = \frac{S}{2} \sum_{\mathbf{r}} [A_{zz} \cos \Theta \cos \theta(\mathbf{R}+\mathbf{r}) + \sin \Theta \sin \theta(\mathbf{R}+\mathbf{r}) \\ \times [\cos \Phi \tilde{A}_{xx} \cos(\phi(\mathbf{R}+\mathbf{r}) + \phi_1) \\ + \sin \Phi \tilde{A}_{yy} \sin(\phi(\mathbf{R}+\mathbf{r}) + \phi_2)],$$

where $\tilde{A}_{xx} = [A_{xx}^2 + A_{xy}^2]^{1/2}$, $\tilde{A}_{yy} = [A_{yy}^2 + A_{yx}^2]^{1/2}$, ϕ_1 and ϕ_2 are phase shifts. It should be noted that the IC structure can be described in different ways, both as a simple plane-wave or as a regular array of domain walls (solitons). If the concentration of solitons is large enough, we arrive at a soliton lattice. Below we assume a plane-wave modulated IC spin state, where the spin modulation phase is a harmonic function of the space coordinate in the direction of the modulation (hereafter Z axis). Such a spiral spin structure we define as follows: $\mathbf{S}(\mathbf{R}) = S(\sin \theta(\mathbf{R}) \cos \phi(\mathbf{R}), \sin \theta(\mathbf{R}) \sin \phi(\mathbf{R}), \cos \theta(\mathbf{R}))$, where $\theta(\mathbf{R}) = k_1 Z + \theta_0$, $\phi(\mathbf{R}) = k_2 Z + \phi_0$ with $k_{1,2}$ being IC spatial modulation wave numbers. In particular cases this spin structure can be reduced to any types of C states including simple FM and AFM ones. In the continuum approximation the resultant NMR line shape for a static case corresponds to the density of the local field distribution $g(Z) \propto |dH(Z)/dZ|^{-1}$ convoluted with the individual line shape.¹⁶ Actually the straightforward application of this procedure is restricted by rather simple particular cases. However, the lack of a central peak and of any other sharp lines in the NMR spectrum at $T=4$ K for all orientations of the ex-

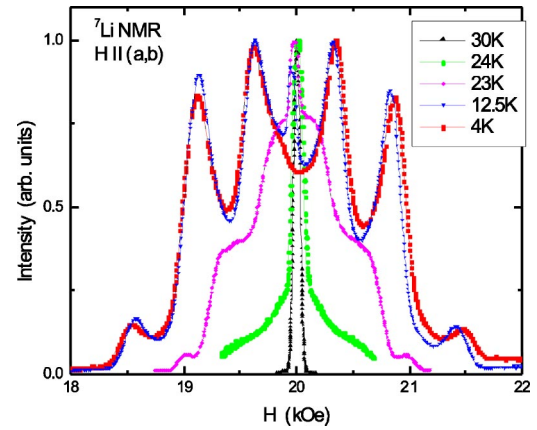


FIG. 2. (Color online) The ${}^7\text{Li}$ NMR spectra taken at various temperatures below the critical temperature of the magnetic ordering. The magnetic field is directed \parallel to the $\mathbf{a}(\mathbf{b})$ axis.

ternal magnetic field points to a spatial modulation of all three spin components. Hence, we are led to consider complex spatial spirals with a modulation of the longitudinal (S_z) as well as of the transversal ($S_{x,y}$) spin components. The specific quartet line shape for the $\mathbf{H} \perp (\mathbf{a}, \mathbf{b})$ geometry and the sextet one for $\mathbf{H} \parallel (\mathbf{a}, \mathbf{b})$, with equivalent signals for $\mathbf{H}_0 \parallel \mathbf{b}$, $\mathbf{H}_0 \parallel \mathbf{a}$, and the field oriented along the diagonal in ab plane, yield constraints for possible types of spirals reducing substantially their number. The measured NMR spectrum can be well described by a simulation assuming a spin spiral twisting along the chain \mathbf{b} axis with identical modulation periods both for the longitudinal and the transversal spin components ($k_1 = k_2$). Within the long-wavelength limit and for a short-range hyperfine coupling the NMR field shift due

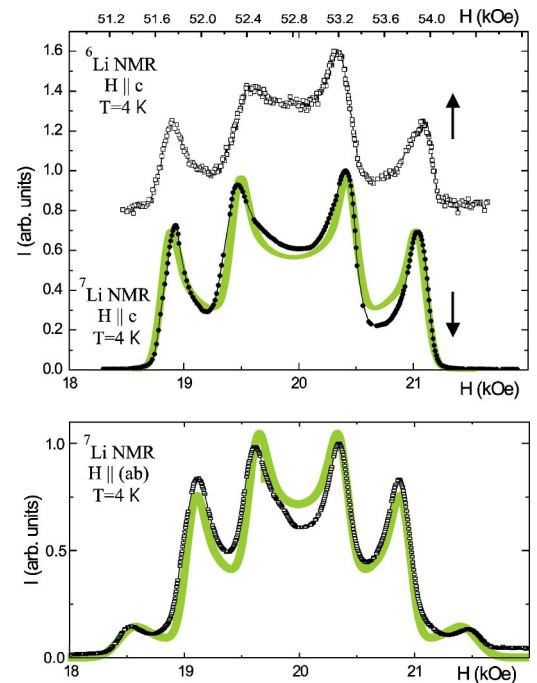


FIG. 3. (Color online) The ${}^6\text{Li}$ and ${}^7\text{Li}$ NMR spectra taken at 4 K. The solid curves in both panels show the results of our theoretical simulation (see the text).

to a (super) transferred hyperfine coupling in $\mathbf{H} \perp (\mathbf{a}, \mathbf{b})$ geometry for the spiral with a “positive” twisting along \mathbf{b} axis ($\mathbf{k} \parallel \mathbf{b}$, or $k > 0$) can be written as follows: $h = (S/4)(\Sigma \tilde{A}_{xx})[\sin(2kZ + \phi_1) - \sin \phi_1]$, where $S \Sigma \tilde{A}_{xx}$ is the maximal value of the hyperfine field for the collinear spin ordering assumed. The spectral density function $g(H)$ has a rather simple form $g(H) \propto [1 - (\omega(H) + \sin \phi_1)^2]^{-1/2}$, with $\omega(H) = 4(H - H_0)/S \tilde{A}_{xx}$. As a result we arrive at two singularities $\omega_{\pm}(H) = \pm 1 - \sin \phi_1$ with a separation $|H_+ - H_-| = (S/2) \tilde{A}_{xx}$ in between, shifted with regard to H_0 by $(S/4) \tilde{A}_{xx} \sin \phi_1$. Taking into account both “positively” ($k > 0$) and “negatively” ($k < 0$) twisted spirals we arrive at a specific symmetric quartet NMR line shape. The situation looks slightly more complex for the “in-plane” geometry, where we deal with two types of twins. For $\mathbf{H}_0 \parallel \mathbf{b}$ or \mathbf{a} axis we arrive at a superposition of two different NMR signals stemming from differently oriented twins, with $\mathbf{H}_0 \parallel \mathbf{Z}$ or $\mathbf{H}_0 \perp \mathbf{Z}$, respectively. The former are described by a simple expression for the NMR frequency shift: $h = (S/2) A_{zz} \cos kZ$ with the well-known symmetric doublet line shape,¹⁶ while the latter yield a NMR response qualitatively similar to that of $\mathbf{H} \perp (\mathbf{a}, \mathbf{b})$ geometry. Thus we arrive at a sextet line shape. Making use of the Gauss convolution procedure¹⁷ we successfully simulate the NMR spectra both for $\mathbf{H} \perp (\mathbf{a}, \mathbf{b})$ and $\mathbf{H} \parallel (\mathbf{a}, \mathbf{b})$ geometry (Fig. 3). It is noteworthy that the current NMR study of IC phase does not yield information regarding both the IC period and the absolute value of the spin order parameter. Nevertheless, the simulation provides valuable insight into the effective (super)transferred Cu(O)-^{6,7}Li hyperfine interactions. In fact, we obtain: $S|\Sigma A_{zz}| \approx S|\Sigma \tilde{A}_{xx}| \approx 3$ kOe, $S|\Sigma \tilde{A}_{yy}| \approx 2.6$ kOe. The large magnitude and closeness of these parameters point to the predominance of covalently enhanced isotropic (super)transferred Li-Cu(O) hyperfine interactions as compared with anisotropic magnetic dipole terms. It should be noted that our current approach implies implicitly a mutual collinear interchain ordering. A more detailed analysis of interchain coupling and impurity effects are challenging problem left for future studies.

The discreteness of the crystal lattice is expected to cause pinning with a tendency to lock in the IC wave vector for a spiral at C values and might give rise to a “Devil’s staircase” type behavior.¹⁶ We hypothesize that LiCu_2O_2 with a series of phase transitions at 24.2, 22.5, and 9 K exhibits such a behavior. This conjecture is supported by the temperature evolution of our NMR spectra (see Fig. 2) which reveals a well developed central peak in a wide temperature range below 24 K. This is a signature of strong low-energy dynamical fluctuations of local magnetic field typical for acoustic-like phase fluctuations, or phasons generic for IC structures. So, the first order phase transition at 9 K may be attributed to pinning effects. Noteworthy the phason-like spin fluctuations may result in a sizeable frequency dependence of the transverse relaxation rate T_2^{-1} affecting strongly the NMR line shape. These effects differ substantially for different singularities in the NMR line shape, in particular, they maybe responsible for the weak intensity of the outer doublet in the NMR spectrum for $\mathbf{H} \parallel (\mathbf{a}, \mathbf{b})$ geometry.

To elucidate the origin of the observed IC spin ordering, the knowledge of the relevant magnetic couplings is essen-

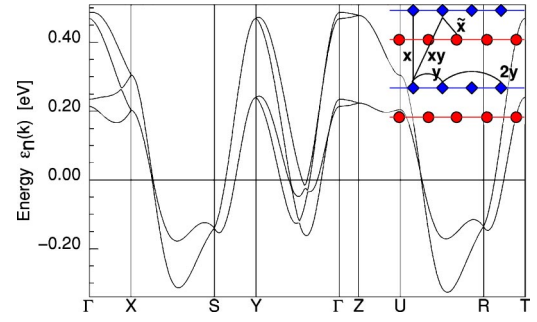


FIG. 4. (Color online) Band structure of LiCu_2O_2 near the Fermi energy, with $\Gamma=(1,0,0)$, $X=(1,0,0)$, $Y=(0,1,0)$, $Z=(0,0,1)$, $R=(1,1,1)$, $S=(1,1,0)$, $T=(0,1,1)$, $U=(1,0,1)$ in units of π/a , π/b , π/c , respectively. The inset shows a sketch of a bilayer with double chains (\bullet and filled \diamond) running along \mathbf{b} together with our notation for the main transfer and exchange processes.

tial, especially with respect to frustrations. In particular, the ratio $\alpha = |J_{nmn}/J_{nn}|$ in a single-chain approach of the FM-AFM J_1 - J_2 -Heisenberg model is decisive for C order ($\alpha < 1/4$) or IC one ($\alpha > 1/4$).³ To estimate the main transfer integrals t and exchange couplings J , we performed full potential LDA calculations using the FPLO code.¹⁹ The resulting bands near the Fermi energy, shown in Fig. 4, have been fitted by an extended tight-binding (TB) model to obtain the t 's. The result is given in Table I. The in-chain dispersion along the k_y directions (Γ - Y) shows deep minima in the middle of BZ indicating the predominance of the nnn transfer over the nn term with $t_{2y} \approx -109$ meV and $|t_y| \approx 64$ meV, respectively. This causes a strong in-chain frustration within the spin-1/2 Heisenberg model $H = \sum_{\langle ij \rangle} J_{ij} \mathbf{S}_i \mathbf{S}_j$. The AFM contributions to the J 's estimated within a single band Hubbard model are given by $J_{ij}^{\text{AFM}} = 4t_{ij}^2/U$. We adopt for the screened on-site repulsion $U = 3$ eV as an appropriate value.⁵ The result is given in Table I. The screened FM Heisenberg contributions J^{FM} (see Table I) have been found using Wannier functions²⁰ of Li_2CuO_2 which is closely related to LiCu_2O_2 with respect to its in-chain geometry and crystal field. The effective exchange J^{eff} is given by the sum of the two former contributions (see Table I). As one may expect for a nearly 90° Cu-O-Cu bond angle according to the Goodenough-Kanamori rule, we arrive at a negative (FM) total nn in-chain exchange $J_y \approx -8.1$ meV,²¹ and at an AFM nnn exchange: $J_{2y} \approx +14.5$ meV. The main interchain transfer process t_x is comparable with the nn term t_y , but the corresponding FM exchange contribution is small resulting in $J_x^{\text{eff}} = 5.7$ meV. For the small transfer terms t_{xy} and $t_{\bar{x}}$, the corresponding FM

TABLE I. LDA derived transfer integrals t and exchange constants J in meV, notation according to inset of Fig. 4.

	y	$2y$	x	\bar{x}	xy
$ t $	64	109	73	18	25
J^{AFM}	5.5	15.8	7.1	0.4	0.8
J^{FM}	-13.6	-1.4	-1.4	-	-
J^{eff}	-8.1	14.4	5.7	0.4	0.8

contributions are expected to be very small and are ignored therefore. From the values in Table I we conclude that LiCu_2O_2 is a quasi-2D system in an electronic sense but magnetically more anisotropic. Using the calculated J 's, we end up with $\alpha \sim 1$ well above the critical ratio of $1/4$. We emphasize that for a $3d$ arrangement of chains such as in LiCu_2O_2 and the FM sign of J_y found, the in-chain frustration is the *only* strong enough source to drive a spiral. Thus LDA provides strong microscopic support for the scenario suggested by the phenomenological NMR analysis. In a more realistic anisotropic multiple chain situation, α_c would be slightly larger. However, with $\alpha \sim 1$ the ignored interchain coupling and spin anisotropy should not change essentially our physical picture. This is at variance with the homogeneous FM in-chain order found in $\text{Ca}_2\text{Y}_2\text{Cu}_5\text{O}_{10}$ ($\alpha=0.05$)⁶ and Li_2CuO_2 ($\alpha < 1$) with much stronger interchain coupling. Hence, LiCu_2O_2 is unique, in being the first realization of a long sought for spiral chain compound on the ferromagnetic nn - J_1 side of the J_1 - J_2 phase diagram. It is one of the most strongly frustrated cuprates we know.

In conclusion, we present the first experimental evidence of a low-temperature IC in-chain spin structure in an undoped quasi-1D cuprate.²² Below 24 K the ^7Li NMR line shape in LiCu_2O_2 presents a clear signature of an IC static modulation of the local magnetic field consistent with a spiral modulation of the magnetic moments twisted along the chain axis. The intrinsic incommensurability accompanied

by pinning effects is believed to be responsible for an unconventional evolution of a low-temperature spin structure with a series of successive phase transitions resembling the “Devil’s staircase” type behavior. Applying an independent extended TB and subsequent Heisenberg analysis based on LDA calculations we succeeded to elucidate a strong in-chain frustration and in this way also the microscopic origin of the magnetic spiral seen by the NMR.

Note added in proof. From $\chi(T)$,¹² we found $J_1 \sim -J_2 = -8.2$ meV, in comparison with refined LDA values $J_1 = -13.9$ and $J_2 = 10.1$ meV, where $U \sim 4$ eV [suggested by a new analysis of $\chi(T)$, XAS, and optical conductivity data of Li_2CuO_2] and a reduced screening factor²⁰ have been used. The extension of our J_1 - J_2 FM-AFM single chain model with respect to the interchain coupling $J_{\bar{x}}$ is straightforward. For both signs, $J_{\bar{x}}$ does not lead to frustration with respect to a FM J_1 and results in moderate quantitative changes, leaving J_2 the microscopic driving force for the helix formation.

We thank A. Vasiliev, J. Richter, J. Málek, W. Ku, and H. Eschrig for fruitful discussions. We appreciate support by Grant Nos. MD-249.2003.02, RFBR 04-03-32876, RFBR 02-02-16369 [A.G.], INTAS 01-0654, CRDF RU-P1-2599-MO-04 [A.G. and E.M.] CRDF REC-005, E 02-3.4-392, UR.01.01.042, RFBR 01-02-96404 [A.M.], DFG (SPP 1073 [S.-L.D.] and Emmy-Noether-program [H.R.]).

*Deceased.

- ¹S. A. Zvyagin, G. Cao, Y. Xin, S. McCall, T. Caldwell, W. Moulton, L.-C. Brunal, A. Angerhofer, and J. E. Crow, *Phys. Rev. B* **66**, 064424 (2002).
- ²K.-Y. Choi, S. A. Zvyagin, G. Cao, and P. Lemmens, *Phys. Rev. B* **69**, 104421 (2004).
- ³T. Hamada, J. Kane, S. Nakagawa, and Y. Natsume, *J. Phys. Soc. Jpn.* **57**, 1891 (1988).
- ⁴V. Ya. Krivnov and A. A. Ovchinnikov, *Phys. Rev. B* **53**, 6435 (1996).
- ⁵Y. Mizuno, T. Toyama, S. Maekawa, T. Osafune, N. Motoyama, H. Eisaki, and S. Uchida, *Phys. Rev. B* **57**, 5326 (1998).
- ⁶M. Matsuda *et al.*, *J. Phys. Soc. Jpn.* **68**, 269 (1999).
- ⁷M. Horvatić, Y. Fagot-Revurat, C. Berthier, G. Dhalenna, and A. Revcolevschi, *Phys. Rev. Lett.* **83**, 420 (1999).
- ⁸S. J. Hibble *et al.*, *J. Solid State Chem.* **88**, 534 (1990).
- ⁹R. Berger *et al.*, *J. Less-Common Met.* **175**, 119 (1991).
- ¹⁰D. A. Zatsopin, V. R. Galakhov, M. A. Korotin, V. V. Fedorenko, E. Z. Kurmaev, S. S. Bartkowski, M. Neumann, and R. Berger *Phys. Rev. B* **57**, 4377 (1998).
- ¹¹B. Roessli *et al.*, *Physica B* **296**, 306 (2001).
- ¹²T. Masuda, A. Zheludev, A. Bush, M. Markina, and A. Vasiliev, *Phys. Rev. Lett.* **92**, 177201 (2004) to be compared with condmat/0310126 by the same authors.
- ¹³F. C. Fritschij *et al.*, *Solid State Commun.* **107**, 719 (1998). These first ^7Li NMR measurements were performed on powder samples in the paramagnetic state, only.
- ¹⁴For details of sample preparation see Ref. 12.
- ¹⁵C. Berthier, D. Jerome, and P. Molinier, *J. Phys. C* **11**, 797 (1978).
- ¹⁶R. Blinc, *Phys. Rep.* **79**, 333 (1981). Strictly speaking, the devil’s stair case scenario has been confirmed theoretically, so far for the simpler ANNI-model, only. Here we suggest its applicability also for the anisotropic Heisenberg model which is more relevant for LiCu_2O_2 .
- ¹⁷M. Kogoj, S. Žumer, and J. Blinc, *J. Phys. C* **17**, 2415 (1984).
- ¹⁸The two lithium isotopes: ^7Li ($I=3/2$; $\gamma=16.55$ MHz/T; $Q=-3.66$ barn) and ^6Li ($I=1$; $\gamma=6.27$ MHz/T; $Q=-0.064$ barn) provide an opportunity to separate magnetic and electric quadrupole hyperfine interactions.
- ¹⁹K. Koepernik and H. Eschrig, *Phys. Rev. B* **59**, 1743 (1999).
- ²⁰W. Ku, H. Rosner, W. E. Pickett, and R. T. Scalettar, *Phys. Rev. Lett.* **89**, 167204 (2002). Calculations for Li_2CuO_2 see: H. Rosner *et al.* (unpublished). The bare interactions amount $U^b = 9.85$ eV, $J_y^{\text{FM},b} = 44.2$ meV, and $J_{2y}^{\text{FM},b} = 4.5$ meV. Since the single band effective $U \approx \Delta \approx 3$ eV (Ref. 5), a screening factor of 3.3 can be estimated resulting in $J_y^{\text{FM}} = -13.6$ meV and $J_{2y}^{\text{FM}} = -1.4$ meV. This way we arrive for Li_2CuO_2 at $J_1^{\text{eff}} = -7.6$ meV and $J_2^{\text{eff}} = 7.3$ meV close to various estimates in the literature.
- ²¹A similar conclusion has been drawn in Ref. 10.
- ²²After the submission of our manuscript, we learned about neutron data (Ref. 12) also pointing to a spiral propagating along b . However, their interpretation in terms of a dimer liquid (Refs. 1 and 2) is based on pure AFM J 's and a planar (ab) spin structure is inconsistent with our results.